Journal of Colloid and Interface Science 466 (2016) 162–167

Contents lists available at ScienceDirect

Journal of Colloid and Interface Science

journal homepage: www.elsevier.com/locate/jcis

# Integrated microfluidic system with simultaneous emulsion generation and concentration

Karuna S. Koppula [a,1], Rong Fan [b,1], Kartik R. Veerapalli [b], Jiandi Wan [b,*]

[a] Department of Chemical Engineering, Rochester Institute of Technology, Rochester, NY 14623, USA
[b] Microsystems Engineering, Rochester Institute of Technology, Rochester, NY 14623, USA

## GRAPHICAL ABSTRACT

An efficient microfluidic emulsion generation system integrated with an orifice structure has been presented to separate aqueous droplets from the continuous oil phase. The efficiency of separation is determined by a balance between pressure drop and droplet accumulation near the orifice. Scale bar: 60 μm.

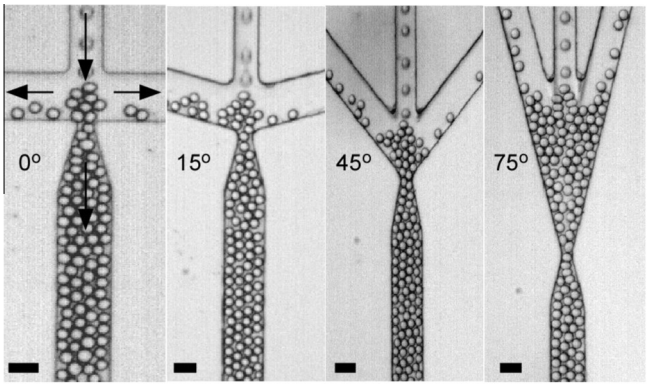


## ARTICLE INFO

*Article history:*
Received 29 October 2015
Revised 11 December 2015
Accepted 17 December 2015
Available online 18 December 2015

*Keywords:*
Microfluidics
Emulsion drops
Emulsion concentration and separation

## ABSTRACT

Because the size, size distribution, and concentration of emulsions play an important role in most of the applications, controlled emulsion generation and effective concentration are of great interest in fundamental and applied studies. While microfluidics has been demonstrated to be able to produce emulsion drops with controlled size, size distribution, and hierarchical structures, progress of controlled generation of concentrated emulsions is limited. Here, we present an effective microfluidic emulsion generation system integrated with an orifice structure to separate aqueous droplets from the continuous oil phase, resulting in concentrated emulsion drops in situ. Both experimental and simulation results show that the efficiency of separation is determined by a balance between pressure drop and droplet accumulation near the orifice. By manipulating this balance via changing flow rates and microfluidic geometry, we can achieve monodisperse droplets on chip that have a concentration as high as 80,000 drops per microliter (volume fraction of 66%). The present approach thus provides insights to the design of microfluidic device that can be used to concentrate emulsions (drops and bubbles), colloidal particles (drug delivery polymer particles), and biological particles (cells and bacteria) when volume fractions as high as 66% are necessary.


* Corresponding author.
*E-mail address:* jdween@rit.edu (J. Wan).
[1] Karuna S. Koppula and Rong Fan contributed equally to this work.

http://dx.doi.org/10.1016/j.jcis.2015.12.032
0021-9797/

## 1. Introduction

Microfluidics has been demonstrated as an effective platform for generation of emulsion droplets [1,2] and plays an important role in manufacture of drugs, food products and synthetic materials in the form of microparticles or microbeads, microgels, and microcapsules [3–5]. Recent advances in microfluidics have yielded unprecedented control over the generation of emulsions and we can now manipulate the producing rate, size distribution, and hierarchical structures of emulsion droplets [6–9]. An ultra-high producing rate of emulsion drops over 1 kg/day, for example, has been achieved using microfluidics [10,11]. Emulsions with hierarchical structures including double emulsion [10], triple emulsion [12], and multicomponent multiple emulsion [13] can also be produced via microfluidic approaches.

The majority of microfluidic approaches, however, produce emulsion drops with a low concentration. This is because, in order to generate droplets with a small diameter (~a few to tens of micrometers), the volumetric flow rate of the continuous phase is usually higher than that of the disperse phase [14], resulting in a low volume fraction of drops in the collection reservoir. As a consequence, significant amount of fluids of the continuous phase is required to produce a relatively large amount of emulsion drops. The large consumption of continuous fluids and low concentration of emulsion drops significantly limit its applications in many fields in which large-scale production of drops is preferred [15]. Strategies that can reduce the amount of continuous fluids and concentrate emulsion drops are thus of great interest. Filtering can separate droplets from the continuous fluids but droplets either will break and/or stick to the filter paper during filtering, resulting in a low harvesting yield. In addition, off-line droplet collection and handling may cause contamination and increased emulsion instability, which are undesired for most of the droplet applications. Active sorting of microfluidic-generated droplets, on the other hand, applies external electric [16], dielectrophoretic [17], or magnetic forces [18] to manipulate droplets individually in desired directions and thus have been demonstrated to be able to achieve high volume fractions of droplets. The need of fabrication of complex interfacing components such as electrodes, piezoelectric and mechanical parts in microfluidics, however, limits its application. Although alternative approaches using different geometry of microchannel [19–21] and surface wetting patterns [22] have been developed to manipulate and sort droplets, most of them rely on the complex geometry design and are used for size-dependent droplet separation. Effective strategies to concentrate emulsion drops still remain to be explored.

Here, we demonstrate a simple yet unique microfluidic device with built in facility for simultaneous generation and concentration of uniform sized aqueous droplets in a continuous oil phase. In particular, a flow-focusing design is used to generate droplets whereas a downstream V-shape junction is used to concentrate droplets. The developed microfluidic platform with simple geometry design enables direct size-dependent separation of droplets from the continuous stream, which avoids the using of external forces and the need of extra off-chip separating step. In addition, the integrated microfluidic system is able to simultaneously generate and concentrate monodisperse droplets with a concentration as high as 80,000 drops per microliter (volume fraction of 66%, drop sizes of ~20 μm) at a relatively low shear stress, i.e., ~12.5 Pa. The demonstrated microfluidic system thus provides a potential platform in which emulsion drops, particles or biological cells can be separated and concentrated in an effective manner, which are advantageous for applications in chemical, biomedical, and pharmaceutical engineering.

## 2. Materials and methods

### 2.1. Device fabrication and experimental setup

PDMS microfluidics is fabricated using the standard soft lithography technique. The setup for the generation of water-in-oil emulsion drops includes a flow focusing junction continuously generating aqueous droplets in a Novec@ HFE 7500 oil phase (3-ethoxy-1,1,1,2,3,4,4,5,5,6,6,6-dodecafluoro-2-trifluoromethyl-hexane, 99%, 3 M) with 2 wt% Krytox 157FSL (Fluorocarbon surfactant with 21.6% carbon, 9.4% oxygen and 69.0% fluorine, DuPont), as shown in Fig. 1A. Deionized water (18 MΩ cm, 100%) is used as the aqueous phase. The width of the channel for aqueous and oil phase is 100 μm and 150 μm, respectively; the width of the central channel where aqueous droplets are dispersed into the oil phase is 60 μm. The height of the channel is equal to 30 μm everywhere. The width of the constriction of the orifice in outlet 3 is 30 μm. The orifice at the entrance of outlet3 has thus a square section (30 × 30 μm). In the experiment, the aqueous and oil phases are loaded into two different syringes connected to syringe pumps (NE 300) and transported from the syringes to the microfluidic devices using polyethylene tubing (PE 20) connected from the syringe needles to the inlet holes of the device. The interfacial tension between water and HFE 7500 oil phase in the presence of Krytox surfactant is approximately 1–5 mM/m [6]. Because the same aqueous and oil phases are used to generate drops, the interfacial tension of drops is the same. In addition, the fluorinated oil used in the experiment wets the PDMS wall [23] and the interfacial tension between the water and oil phase in the presence of Krytox surfactant is low, surface energy has thus a minor impact on the drop concentration. The generated drops are stable throughout the experiment and during droplet collection, which takes approximately 3–4 h. The aqueous and oil phases have the density of 1 kg/m$^3$ and 1614 kg/m$^3$, respectively. Water-in-oil emulsion drops are used for all the experiments. The typical Reynolds number in our experiments is from 15 to 78.

### 2.2. Image analysis

Generation of droplets is observed using a high-speed video camera (Phantom, Micro M110) mounted on a microscope (Leica). The exit velocity of the droplets and their respective diameters are analyzed using an image analysis program written in Matlab. An algorithm is used to track and count the number of droplets entering the central channel and track the exit path they take in each given device. It uses distance and Hough transforms with image morphological operations to track each droplet's path over a set of frames in the given video of the process. As the accuracy of this algorithm is highly dependent on the video quality of the process, wavelet based de-noising is performed on each of the video frames.

## 3. Results and discussion

An illustration of the integrated V-junction microfluidic device is shown in Fig. 1A. Aqueous droplets are generated in a continuous oil phase using a flow-focusing design and exit through three outlets, namely, outlet 1, 2 and 3. In a typical experimental setup, it has been observed that the majority of the dispersed droplets exit through outlet 3 while the continuous oil phase exits through outlets 1 and 2 (Fig. 1B), resulting in an effective separation of the emulsion droplets from the continuous phase. This observation of passive hydrodynamic separation of emulsion drops triggers the mechanistic investigation of the effect of flow parameters and design factors on the separation. In particular, the effects of (i) oil-to-water flow rate ratio ($Q_o/Q_w$), and (ii) angles of orientation

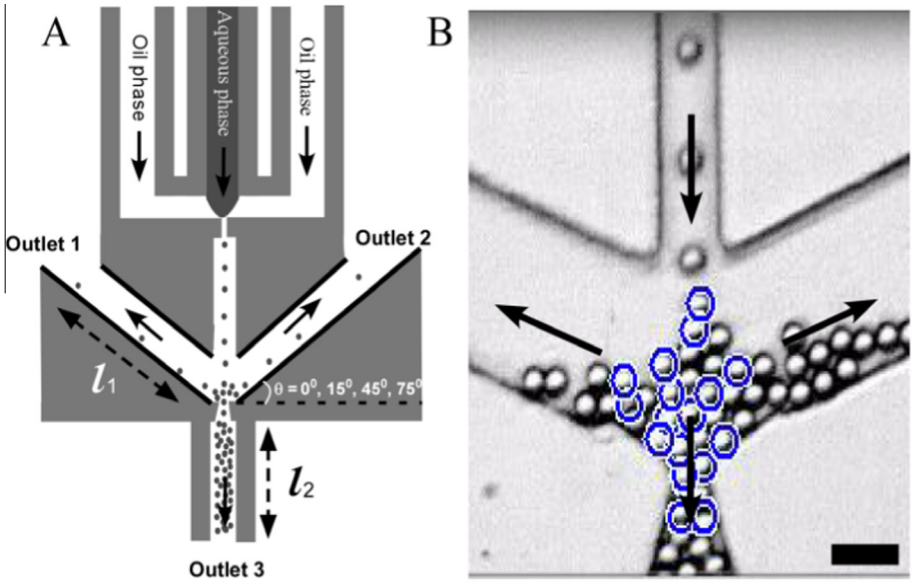


**Fig. 1.** Microfluidic approach to separate emulsion drops. (A) Schematic of the experimental apparatus (not to scale). Water-in-oil drops are generated using flow-focusing microfluidics and then exit through three outlets. Outlet 1 and 2 are the side-exiting channels and have the same flow resistance (i.e., the same length of $l_1$) and angles ($\theta$) of 0°, 15°, 45° or 75° relative to the horizontal direction. In the experiments, the majority of continuous phase is exited through outlet 1 and 2. Outlet 3 is the channel where drops are concentrated and has a length of $l_2$. (B) Representative experimental image of concentrating drops in microfluidics. The number of drops flowing into different outlets is labeled with a blue circle and tracked using an image analysis program written in-house with Matlab software. Arrows indicate the flow direction of drops. $\theta = 15°$, water flow rate ($Q_w$) is 2 μl/min, oil flow rates ($Q_o$) is 28 μl/min. Scale bar: 60 μm. (For interpretation of the references to color in this figure legend, the reader is referred to the web version of this article.)

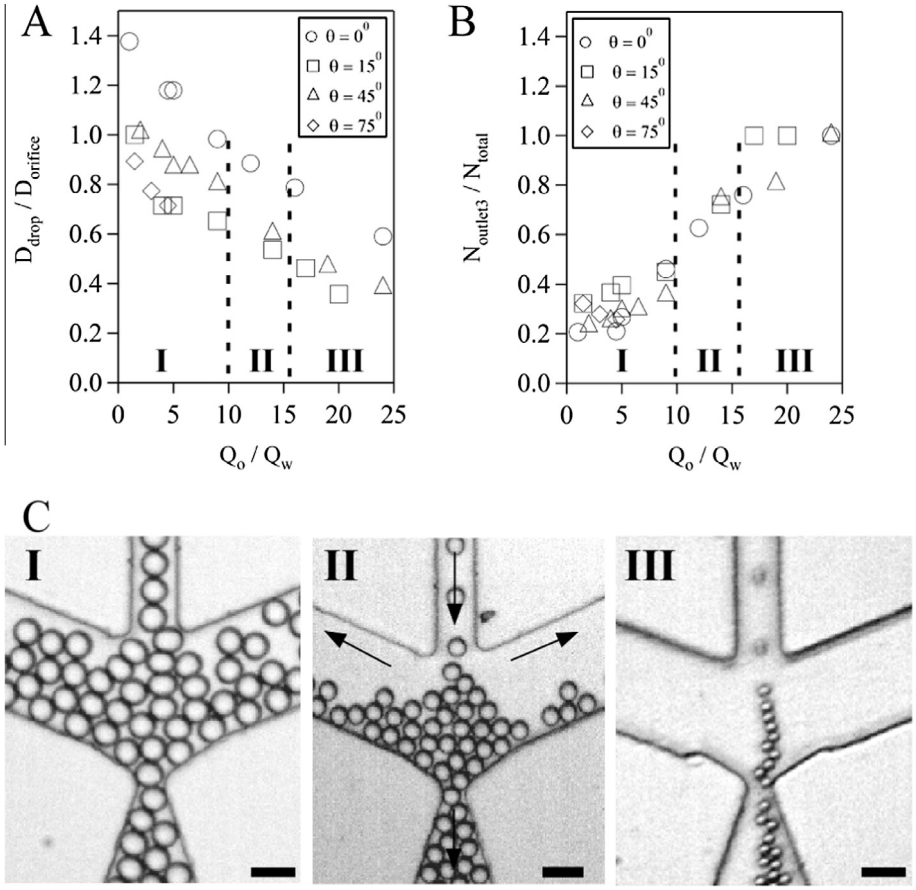


**Fig. 2.** Effect of oil-to-water flow rate ratio ($Q_o/Q_w$) on the concentrating of emulsion drops. (A) Variation in the size ratio between drops and width of the orifice ($D_{drop}/D_{orifice}$) with $Q_o/Q_w$ in microfluidic devices ($l_1$ = 17,848 ± 1799 μm, $l_2$ = 42,042 ± 949 μm, and $\theta$ = 0°, 15°, 45° and 75°). (B) Variation of the fraction of drops exiting through outlet 3 ($N_{outlet3}/N_{total}$) with $Q_o/Q_w$. (C) Snapshots of droplets exiting through outlet 3 and side-exiting channels at $D_{drop}/D_{orifice}$ = 1 (I), 0.6 (II), and 0.4 (III), which corresponds to $Q_o/Q_w$ of 1.5, 14, and 20, respectively. $\theta$ = 15°. Arrows indicate the direction of flow. Note that although high $N_{outlet3}/N_{total}$ can be achieved by increasing $Q_o/Q_w$, $D_{drop}/D_{orifice}$ decreases at high $Q_o/Q_w$. Consequently, considerable amount of continuous phase flows into the outlet 3 and the concentration of drops in outlet 3 decreases, as shown in III. Scale bar: 60 μm.

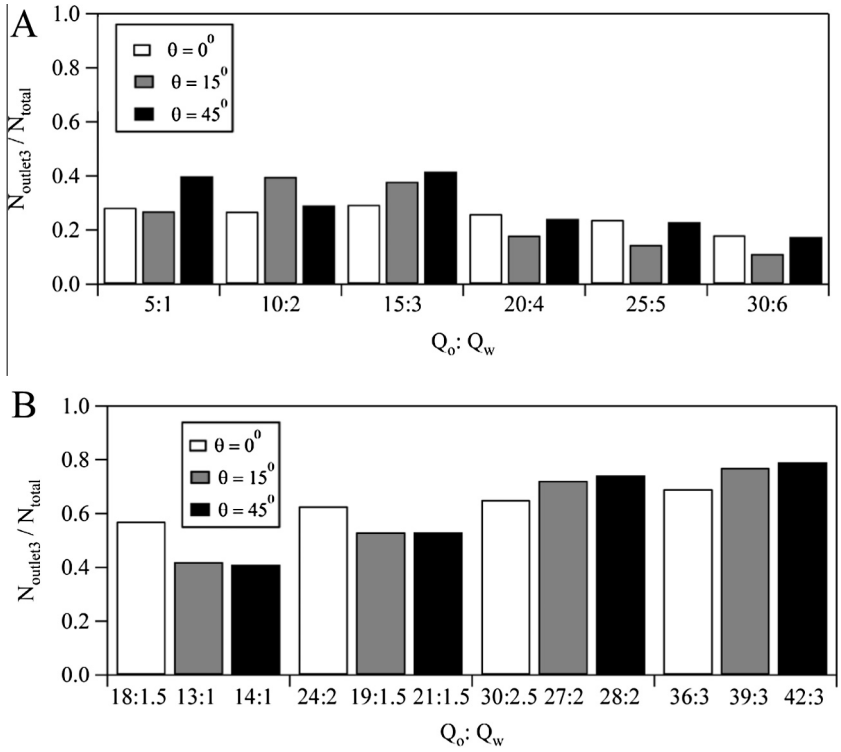


**Fig. 3.** Effect of total flow rates on the fraction of drops exiting through outlet 3 ($N_{outlet3}/N_{total}$). (A) Dependence of $N_{outlet3}/N_{total}$ on increased total flow rates while the ratio of oil-to-water flow rates ($Q_o/Q_w$) is kept constant ($Q_o/Q_w = 5$) and (B) $Q_o/Q_w \approx 13$.

of the outlets 1 & 2 ($\theta$) on emulsion generation and concentration are studied. Because V-junction microfluidics has been used recently for the generation of drug delivery polymer nanoparticles [24–26], understanding of the effect of flow and geometric factors on separation of emulsion drops in the integrated V-junction microfluidic device is expected to inspire novel and much needed approaches to concentrate drug delivery particles.

When the flow resistance in outlet 3, which is quantified by the length of the channel, is higher than that in outlet 1 and 2, i.e., $l_2 > l_1$, we find that there are three regimes of $Q_o/Q_w$ that greatly impact the separation process (Fig. 2). In regime I, $Q_o/Q_w$ is relatively small ($Q_o/Q_w < 10$), and the diameter of aqueous droplets ($D_{drop}$) is either greater than or comparable to the hydraulic diameter of the orifice at the entrance of outlet 3 ($D_{orifice}$) (Fig. 2A). As a result, large droplets tend to trap and accumulate significantly near the orifice and block outlet 3 (Fig. 2C, I). The exit fraction, $N_{outlet3}/N_{total}$ that is defined as number of droplets exiting through the outlet 3 relative to the total number of droplets exiting through all the outlets, is less than or equal to 0.5 (Fig. 2B). When $Q_o/Q_w$ is greater than 16 (regime III), the droplet size is smaller than the orifice size ($D_{drop}/D_{orifice} \leqslant 0.5$). Thus, almost all the droplets exit straight through the outlet 3, resulting in a high exit fraction ($N_{outlet3}/N_{total} = 1$). However, the separation of emulsion droplets from the continuous oil phase is not effective, as most of the continuous oil phase also exits through the outlet 3 (Fig. 2C, III). For the case when $Q_o/Q_w$ is between 10 and 16 (regime II), the droplet sizes are slightly smaller than the orifice with $0.5 < D_{drop}/D_{orifice} < 0.7$ as can be seen in regime II in Fig. 2A. Separation of emulsion is observed to be most effective in this regime with exit fractions greater than 0.5 and also having less continuous phase through outlet 3. The results demonstrate that $Q_o/Q_w$ plays an important role in the separation process by controlling $D_{drop}/D_{orifice}$. It should be noted that the effect of angles of outlet 1 and 2 ($\theta$) on the separation is not significant in the current experimental setup. In addition, because the density of the continuous oil phase (1614 kg/m$^3$) is much higher than that of the aqueous phase (1 kg/m$^3$), sedimentation is not important in the current separation device. Indeed, even when silicon or mineral oil are used as the continuous oil phase, the sedimentation speed of the drops ($\sim 10^{-10}$–$10^{-9}$ m/s) is much slower than the flow velocity ($\sim 10^{-1}$ m/s) (Table S1 & S3), the time for drops to sediment is much longer than the typical time it takes for drops to move through the V shape. As a result, the effect of sedimentation is expected to be negligible.

On the other hand, we notice that, in regimes I and II, the rate of droplets exiting through outlets 1, 2 or 3 is lower than the rate of droplets arriving at the orifice, which leads to a net increase of the numbers of drops near the orifice at a given time. Accumulation of drops at the orifice thus occurs. Intuitively, a reasonable accumulation of droplets prevents the continuous phase from entering exit 3 while significant accumulation jeopardizes the separation process by blocking the orifice. Thus, effective regulation of the accumulation process near the orifice is likely able to improve the separation efficiency. We thus examine the dependence of exit fractions on the overall $Q_o/Q_w$. In particular, we keep $Q_o/Q_w$ constant but increase the overall flow rates, i.e., the sum of $Q_o$ and $Q_w$ is increased for both regimes I&II. In this case, the size of drops does not change (because $Q_o/Q_w$ is constant) but the pressure drop across the orifice increases due to the increased flow rates. The results show that in regime I where $Q_o/Q_w = 5$, increased flow rates do not seem to have any desired effect (Fig. 3A). This is probably due to the increased generation rate of droplets whose sizes are much larger than or equal to the size of orifice, resulting in a further accumulation of drops near the orifice. However, when the droplet size is about midrange ($0.5 < D_{drop}/D_{orifice} < 0.7$, $Q_o/Q_w \approx 13$), such as in regime II, the increased flow rates have a preferable effect on exit fractions (Fig. 3B), suggesting that the increased overall flow rates in regime II help forcing the droplets

through the orifice more effectively and obtaining a higher exit fraction. Furthermore, the angle ($\theta$) of the outlets 1 and 2 also starts to affect the separation process. For example, exit fraction for devices with $\theta = 15°$ and 45° have a considerable increase in the exit fractions with increasing flow rates (Fig. 3B). In both regimes increased flow rates result in a significant accumulation of drops in devices with $\theta = 75°$, which block the orifice completely and make the separation negligible. Note that the *x*-axis in Fig. 3 shows the actual values of oil flow rate and water flow rate. For example, 15:3 indicates the oil flow rate is 15 μl/min whereas water flow rate is 3 μl/min. There was no significant effect of accumulation of drops on the size of generated drops observed in our experiments.

When the flow resistance in outlet 3 is comparable to that in outlet 1 and 2, i.e., $l_2 \approx l_1$, the angle ($\theta$) of the outlets 1 and 2 starts to affect the droplet accumulation and exit fraction. For devices with 0° and 15° angles, for example, the droplets do not accumulate significantly (~10 droplets) before the orifice regime and tend to leave through the exits 1 & 2 (Fig. 4A). The 45° angle has a considerable accumulation (~20–30 droplets) at any given time. For devices with 75° angle, however, there is a large regime of trapped droplets before the constriction (~60–70 droplets). Because simulation has shown that for devices with 45° and 75° angles there are pockets of low velocity regimes before the orifice, these pockets of low velocity regimes is likely responsible for the observed accumulation of droplets in Fig. 4A (Fig. S1A). Thus, it is possible that $\theta$ regulates the accumulation of droplets near the orifice by controlling the local low velocity regimes. Furthermore, experimental data indicate that the exit fractions in regime II seem to be greater for the device with 45° compared to all the other angles (Fig. 4B), solid triangle symbols in the dotted box highlighting regime II). A 45° angle device has lower accumulation of droplets and is aided by appropriate pressure drop to achieve greater exit fractions than 75° device which has too much accumulation preventing droplet exit even when there is relatively higher pressure (Fig. S1B). Thus, devices with 45° angle seem to have the optimum or desired accumulation of droplets (via the generation of local low velocity regimes) and sufficient pressure to drive droplets through the exit 3. Highly concentrated emulsions, for example, ~80,000 per microliter can be produced with a relatively low shear stress of 12.5 Pa in a 45° angle device (Fig. S2, Table S2 & S3). It should be noted that although the angle ($\theta$) has a considerable effect on the separation of droplets from the continuous phase, any geometric modification of the device that could change the pressure drop across the orifice and droplet accumulation around the orifice will affect the separation process. As a result, the conditions may vary for the T-junction, Y-shape microfluidics and/or additional constriction channels. In addition, other parameters such as surface tension and the size of orifice may play roles in the separation process.

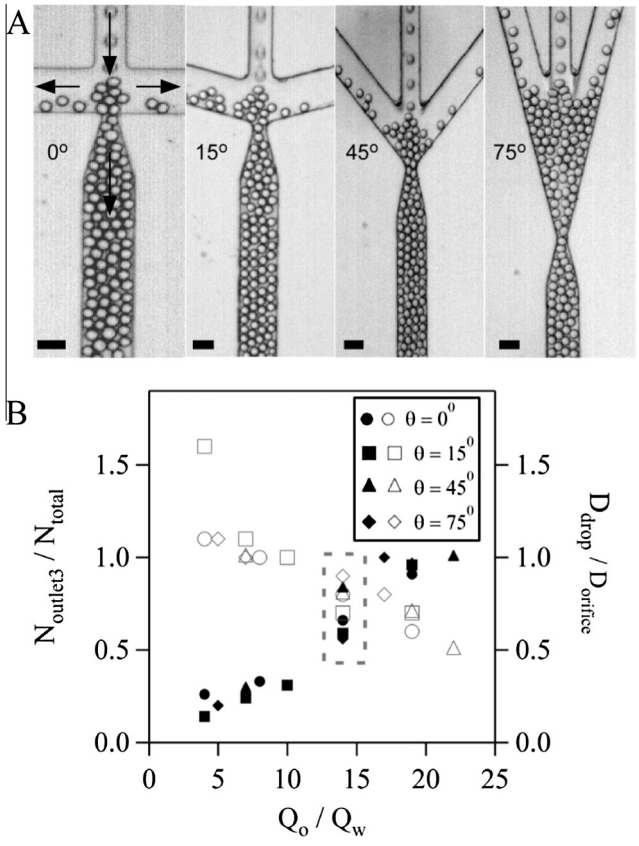


**Fig. 4.** Effect of $\theta$ on the separation of drops using microfluidic devices with $l_1 = 2634 \pm 169$ μm, $l_2 = 2604 \pm 100$ μm. (A) Experimental images of drops flowing in microfluidics with different $\theta$. Arrows indicate the directions of flow. Scale bar: 60 μm. (B) Dependence of the fraction of drops exiting through outlet 3 ($N_{outlet3}/N_{total}$) (solid symbols) and the ratio of droplet diameter to the width of the orifice ($D_{drop}/D_{orifice}$) (empty symbols) on $Q_o/Q_w$. The effect of $\theta$ on $N_{outlet3}/N_{total}$ is highlighted in the box with dot lines.

## 4. Conclusions

In summary, we have developed an integrated V-junction microfluidic system for separation of droplets from the continuous phase. We demonstrated that the separation efficiency depended on the ratio of flow rates, accumulation of droplets near the orifice, and the pressure drop across the orifice. Significant angle effects, which appeared when the flow resistance was comparable for all outlets, were ascribed to the change of local velocity and pressure near the orifice. The 45° angle seemed to be the optimum choice for producing concentrated emulsions (volume fraction of 66%, drop sizes of ~20 μm) with the maximum $N_{outlet3}/N_{total}$. This simple yet unique microfluidic device thus enables direct concentration of droplets from the continuous stream and avoids the using of external forces [16–18] and the need of extra off-chip separating step. In addition, the current approach provides useful guidelines to design microfluidics for concentration of emulsion droplets, and may find many other applications including concentration of microbubbles generated by electrohydrodynamics atomization [27] or pressurized gyration [28,29]. Apart from using this device as an integrated unit for generation of droplets and concentrating emulsions, future work can also be directed to the separation and concentration of particles and biological cells such as blood cells and bacteria.

## Acknowledgements

The authors gratefully acknowledge the support of the Rochester Institute of Technology. J. Wan also acknowledges the Donors of the American Chemical Society Petroleum Research Fund for partial support of this research.

## Appendix A. Supplementary material

Supplementary data associated with this article can be found, in the online version, at http://dx.doi.org/10.1016/j.jcis.2015.12.032.

## References

[1] J.E. Silpe, J.K. Nunes, A.T. Poortinga, H.A. Stone, Generation of antibubbles from core-shell double emulsion templates produced by microfluidics, Langmuir 29 (2013) 8782–8787.

[2] J. Li, H. Chen, H.A. Stone, Breakup of double emulsion droplets in a tapered nozzle, Langmuir 27 (2011) 4324–4327.
[3] C. Zhao, Multiphase flow microfluidics for the production of single or multiple emulsions for drug delivery, Adv. Drug Deliv. Rev. 65 (2013) 1420–1446.
[4] S. Neethirajan, I. Kobayashi, M. Nakajima, D. Wu, S. Nandagopal, F. Lin, Microfluidics for food, agriculture and biosystems industries, Lab Chip 11 (2011) 1574–1586.
[5] A.M. Ganan-Calvo, J.M. Montanero, L. Martin-Banderas, M. Flores-Mosquera, Building functional materials for health care and pharmacy from microfluidic principles and flow focusing, Adv. Drug Deliv. Rev. 65 (2013) 11–12.
[6] A.R. Abate, J. Thiele, D.A. Weitz, One-step formation of multiple emulsions in microfluidics, Lab Chip 11 (2011) 253–258.
[7] J. Wan, A. Bick, M. Sullivan, H.A. Stone, Controllable microfluidic production of microbubbles in water-in-oil emulsions and the formation of porous microparticles, Adv. Mater. 20 (2008) 3314–3318.
[8] H. Chen, Y. Zhao, J. Li, M. Guo, J. Wan, D.A. Weitz, H.A. Stone, Reactions in double emulsions by flow-controlled coalescence of encapsulated drops, Lab Chip 11 (2011) 2312–2315.
[9] L. Rosenfeld, T. Lin, R. Derda, S.K.Y. Tang, Review and analysis of performance metrics of droplet microfluidics system, Microfluid. Nanofluid. 16 (2014) 921–939.
[10] M.B. Romanowsky, A.R. Abate, A. Rotem, C. Holze, D.A. Weitz, High throughput production of single core double emulsions in a parallelized microfluidic device, Lab Chip 12 (2012) 802–807.
[11] J.J. Agresti, E. Antipov, A.R. Abate, K. Ahn, A.C. Rowat, J. Baret, M. Marquez, A.M. Klibanov, A.D. Griffiths, D.A. Weitz, Ultrahigh-throughput screening in drop-based microfluidics for directed evolution, Proc. Natl. Acad. Sci. USA 107 (2010) 4004–4009.
[12] H. Chen, J. Li, J. Wan, D.A. Weitz, H.A. Stone, Gas-core triple emulsion for ultrasound triggered release, Soft Matter 9 (2013) 38–42.
[13] W. Wang, R. Xie, X. Ju, T. Luo, L. Liu, D.A. Weitz, L. Chu, Controllable microfluidic production of multicomponent multiple emulsions, Lab Chip 11 (2011) 1587–1592.
[14] T. Ward, M. Faivre, M. Abkarian, H.A. Stone, Microfluidic flow focusing: drop size and scaling in pressure versus flow-rate-driven pumping, Electrophoresis 26 (2005) 3716–3724.
[15] D. Guzey, D.J. McClements, Formation, stability and properties of multilayer emulsions for application in the food industry, Adv. Colloid Interface Sci. 128 (2006) 227–248.
[16] D.R. Link, E.G. Morgrain, A. Duri, F. Sarrazin, Z. Cheng, G. Cristobal, M. Marquez, D.A. Weitz, Electric control of droplets in microfluidic device, Angew. Chem. Int. Ed. 45 (2006) 2556–2560.
[17] S. Hung, Y. Lin, G. Lee, A microfluidic platform for manipulation and separation of oil-in-water emulsion droplets using optically induced dielectrophoresis, J. Micromech. Microeng. 20 (2010) 045026.
[18] J. Dorvee, A. Derfus, S. Bhatia, M. Sailor, Manipulation of liquid droplets using amphiphilic, magnetic one-dimensional photonic crystal chaperones, Nat. Mater. 3 (2004) 896–899.
[19] Y. Tan, J.S. Fisher, A.I. Lee, V. Cristini, A.P. Lee, Design of microfluidic channel geometries for the control of droplet volume, chemical concentration, and sorting, Lab Chip 4 (2004) 292–298.
[20] H. Maenaka, M. Yamada, M. Yasuda, M. Seki, Continuous and size-dependent sorting of emulsion droplets using hydrodynamics in pinched microchannels, Langmuir 24 (2008) 4405–4410.
[21] L. Mazutis, A.D. Griffiths, Preparation of monodisperse emulsions by hydrodynamic size fabrication, Appl. Phys. Lett. 95 (2009) 204103.
[22] A.R. Abate, A.T. Krummel, D. Lee, M. Marquez, C. Holtze, D.A. Weitz, Photoreactive coating for high-contrast spatial patterning of microfluidic device wettability, Lab Chip 8 (2008) 2157–2160.
[23] H. Boukellal, S. Selimovic, Y. Jia, G. Cristobal, S. Fraden, Simple, robust storage of drops and fluids in a microfluidic device, Lab Chip 9 (2009) 331–338.
[24] I. Kucuk, Z. Ahmad, M. Edirisinghe, M. Orlu-Gul, Utilization of microfluidic V-junction device to prepare surface itraconazole adsorbed nanospheres, Int. J. Pharm. 472 (2014) 339–346.
[25] I. Kucuk, M. Edirisinghe, Microfluidic preparation of polymer nanospheres, J. Nanopart. Res. 16 (2014) 1–9.
[26] I. Kucuk, M. Edirisinghe, Changing the size and surface roughness of polymer nanospheres formed using a microfluidic technique, JOM 67 (2015) 811–817.
[27] S. Mahalingam, M.B.J. Meinders, M. Edirisinghe, Formation, stability, and mechanical properties of bovine serum albumin stabilized air bubbles produced using coaxial electrohydrodynamic atomization, Langmuir 30 (2014) 6694–6703.
[28] S. Mahalingam, B.T. Raimi-Abraham, D.Q.M. Craig, M. Edirisinghe, Formation of protein and protein-gold nanoparticle stabilized microbubbles by pressurized gyration, Langmuir 31 (2014) 659–666.
[29] S. Mahalingam, Z. Xu, M. Edirisinghe, Antibacterial activity and biosensing of PVA-lysozyme microbubbles formed by pressurized gyration, Langmuir 31 (2015) 9771–9780.